Manufacture of a 1.7 m prototype of the GMT primary mirror segments

H. M. Martin[a], J. H. Burge[a,b], S. M. Miller[a], B. K. Smith[a], R. Zehnder[b], C. Zhao[b]

[a]Steward Observatory, University of Arizona, Tucson, AZ 85721, USA
[b]College of Optical Sciences, University of Arizona, Tucson, AZ 85721, USA

ABSTRACT

We have nearly completed the manufacture of a 1.7 m off-axis mirror as part of the technology development for the Giant Magellan Telescope. The mirror is an off-axis section of a 5.3 m f/0.73 parent paraboloid, making it roughly a 1:5 model of the outer 8.4 m GMT segment. The 1.7 m mirror will be the primary mirror of the New Solar Telescope at Big Bear Solar Observatory. It has a 2.7 mm peak-to-valley departure from the best-fit sphere, presenting a serious challenge in terms of both polishing and measurement. The mirror was polished with a stressed lap, which bends actively to match the local curvature at each point on the mirror surface, and works for asymmetric mirrors as well as symmetric aspheres. It was measured using a hybrid reflective-diffractive null corrector to compensate for the mirror's asphericity. Both techniques will be applied in scaled-up versions to the GMT segments.

Keywords: telescopes, optical fabrication, optical testing, aspheres

1. INTRODUCTION

The primary mirror of the Giant Magellan Telescope (GMT) is made of seven 8.4 m circular segments.[1,2] The segments are honeycomb sandwich mirrors produced by the Steward Observatory Mirror Lab, similar to the primary mirrors of the MMT, Magellan telescopes, and Large Binocular Telescope (LBT).[3] The GMT's focal length is 18 m (f/0.7 over the 25.4 m aperture that includes the segments), leading to a compact and stiff telescope structure with a lightweight truss supporting the secondary mirror. The six off-axis segments of this fast primary mirror have asphericity of 14 mm peak-to-valley, and their manufacture presents a challenge. The Mirror Lab has developed a method of polishing highly aspheric mirrors that is expected to produce a figure accuracy for the GMT segments similar to that of the LBT primary mirrors.[4,5] The University of Arizona has developed a number of techniques for measuring aspheric surfaces, many of which involve computer-generated holograms.[6] These techniques form the basis for a set of measurements that have been designed for the GMT segments.[7,8]

The GMT project has undertaken the manufacture of the first off-axis segment. The blank has been cast and the rear surface is being processed, while the Mirror Lab prepares to install a 28 m test tower that will support the measurements. As part of the development for making the GMT segments, we have nearly completed the manufacture of a 1.7 m off-axis mirror which is approximately a 1/5 scale model of the GMT segment. This mirror will be the primary mirror of the New Solar Telescope (NST) at Big Bear Solar Observatory.[9] It has been polished with a 30 cm stressed-lap polishing tool similar to the 1.2 m laps that will be used for the GMT segments. It has been measured using some of the same techniques to be used for the GMT segments, including a hybrid reflective-diffractive null corrector that compensates for the aspheric departure and allows a full-aperture interferometric measurement.

2. THE NST PRIMARY MIRROR

The dimensions of the GMT and NST mirrors are listed in Table 1 for comparison. The NST mirror is 100 mm thick, solid Zerodur, a difference that has little impact on the technology development for GMT. Both the NST mirror and the GMT segment will have active support systems in the telescope, so low-order aberrations such as astigmatism have relaxed tolerances. The NST mirror is supported by 36 actuators in the telescope. For polishing and measurement in the lab, the actuators are replaced by passive hydraulic cylinders whose forces match the operational support forces for zenith-pointing.

Table 1. Dimensions of the off-axis GMT segment and the NST primary mirror.

mirror	diameter	radius of curvature	conic constant	off-axis distance	p-v aspheric departure
GMT segment	8.4 m	36.0 m	-0.99829	8.71 m	14 mm
NST primary	1.7 m	7.7 m	-1	1.84 m	2.7 mm

One of the challenges of making an off-axis mirror is control of the geometry, in particular the radius of curvature, off-axis distance, and clocking angle (rotation of the mirror about its mechanical axis). This control is especially critical for the GMT segments because the radii of the seven segments must match to high accuracy in the telescope, and their support cells—fixed in the telescope—allow only small adjustments in lateral position of the segments. Even without such tight tolerances, measuring the geometry of an asymmetric mirror is more challenging than measurement of a symmetric mirror and requires development of new techniques. For the NST measurements, we rely heavily on position measurements made with a laser tracker, as described in Section 4.2, coupled with simultaneous measurements of the mirror figure to determine the optical aberrations. Requirements for accuracy of measurement of these parameters are listed in Table 2.

Table 2. Requirements for accuracy of measurement of the geometry of the off-axis GMT segment and the NST primary mirror. Values in parentheses are goals for GMT.

parameter	measurement accuracy	
	GMT segment	NST primary
radius of curvature	0.5 (0.3) mm	1.0 mm
off-axis distance	2.0 (1.0) mm	1.0 mm
clocking angle	0.25 mrad	0.6 mrad

3. FABRICATION

The aspheric surface was generated to an accuracy of about 15 µm rms by ITT Industries. Loose-abrasive grinding and polishing were performed by the Mirror Lab. We polished the mirror primarily using a 30 cm diameter stressed lap, essentially the same system used to polish the 1.8 m f/1 primary mirror of the Vatican Advanced Technology Telescope and secondary mirrors for the 3.5 m ARC telescope, 2.5 m Sloan Digital Sky Survey telescope, MMT (three secondaries) and the LBT (two secondaries). The stressed lap changes shape actively to follow the local curvature of the mirror surface. It consists of a 13 mm thick aluminum plate with actuators around its perimeter that apply bending and twisting moments. The plate is stiff enough to provide strong passive smoothing of errors with periods less than about 100 mm. Errors on larger scales are addressed by varying the lap's dwell time, rotation rate, and pressure. This method is augmented by local polishing with passive laps of 50-100 mm diameter.

The stressed-lap polishing system works equally well for axisymmetric and non-axisymmetric mirrors. The lap's ability to polish a given surface depends on the amount it has to bend in order to follow the curvature variations of that surface. The asphericity of the NST mirror has a large amplitude but is dominated by astigmatism and coma, which have relatively small curvature variations, as shown in Figure 1. The required bending of the lap is only about 5% of the full amplitude of asphericity, a much lower ratio than would apply to an axisymmetric mirror whose asphericity is spherical aberration. The lap bending required for the NST mirror is less than the bending required for several of the secondary mirrors that have been figured to high accuracy using the same lap. For the same reason, the GMT segments can be polished with a 1.2 m stressed lap that was designed for axisymmetric primary mirrors with only 1/10 of the asphericity of a GMT segment.
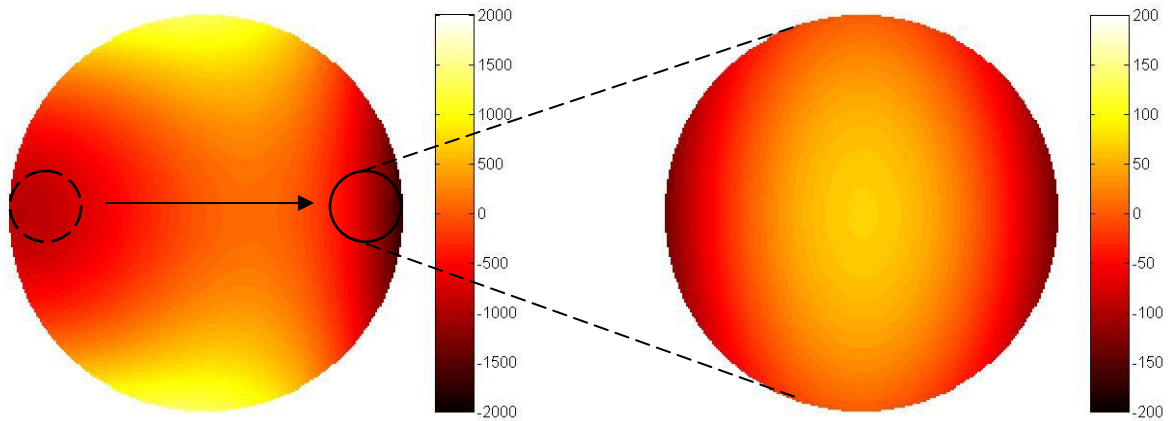
Figure 1. Representation of the asphericity of the 1.7 m mirror (left), and the bending of the 30 cm stressed lap as it moves from one edge of the mirror to the opposite edge (right). Color bars are labeled in μm; note the factor-of-ten difference in scales.

We used the stressed lap for loose-abrasive grinding in order to remove subsurface damage and improve the figure accuracy to about 1 μm rms surface. During this phase we measured the surface with a laser tracker as described in Section 4.1. We then polished and figured the surface with the stressed lap and small passive tools. During both loose-abrasive grinding and polishing, we figured the mirror using the same type of polishing strokes that would be used for an axisymmetric mirror. The lack of symmetry in the surface is taken up entirely by the bending of the stressed lap, with an amplitude of only a few hundred μm as seen in Figure 1. An observer would not discern that the mirror being polished is off-axis.

Figure 2 shows two views of the NST mirror. The photo at left shows the mirror shortly after delivery from ITT. We bonded 36 invar pucks to the rear surface to interface to the support system in the telescope as well as the polishing support seen in the photo. Before polishing began, we developed techniques and software to measure the surface with the laser tracker. The photo at right shows the mirror being polished.
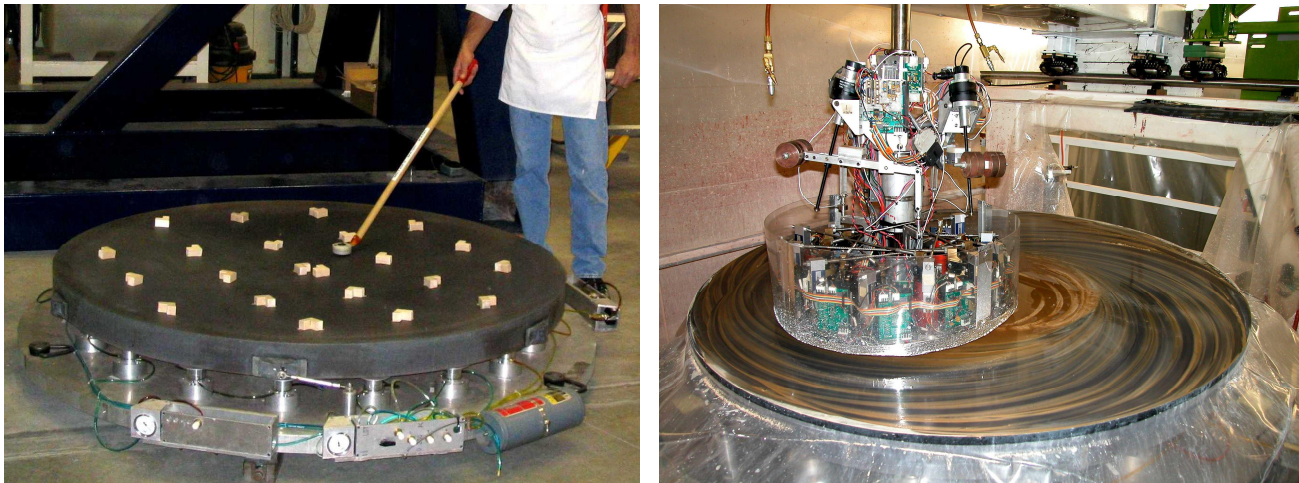

Figure 2. Two views of the NST mirror. Left: resting on its polishing support, before polishing, while a technician practices measuring the surface with a laser tracker. Right: being polished with the 30 cm stressed lap.

4. MEASUREMENTS

4.1 Laser tracker measurements

For symmetric mirrors up to 2 m in diameter, we measure the ground surface with a swing-arm profilometer that makes a one-dimensional scan roughly across a diameter of the mirror. The profilometer can measure asphericity to an accuracy of about 50 nm rms, but it is relatively insensitive to average curvature (power). For the off-axis mirror, the profilometer cannot measure the difference in sag between the two orthogonal diameters (46.0 mm vs 43.5 mm) to an accuracy of a few μm, as is needed to make the transition from loose-abrasive grinding to polishing and testing at 633 nm.

We decided to measure the ground surface with a commercial laser tracker, which combines a distance-measuring interferometer with angular encoders and servos so that it can track a moving retroreflector and measure its position in three dimensions. The retroreflector is mounted in a steel ball with its vertex near the center of the ball, so the tracker measures to a point at a fixed distance (the ball radius) away from any surface. The distance-measuring interferometer measures displacements of a fraction of a μm, but the advertised accuracy of the angular encoders was about 1 arcsecond at the time we purchased the tracker. This would correspond to a position error of about 10 μm over the roughly 2 m distance required to measure the surface of the NST mirror. If the tracker is placed near the mirror's center of curvature, however, the measurement is not very sensitive to angular errors.

We tested three commercial trackers by measuring the figure of a 1.8 m spherical mirror with $R = 10$ m from its center of curvature. All three showed the surface to be accurate to less than 2 μm rms, which means the trackers were accurate to better than 2 μm rms in this favorable geometry. Furthermore, we found that the accuracy was not degraded significantly by moving the tracker to a distance of 3 m from the mirror. (This distance results in a maximum angle of incidence of 12° for the tracker beam at the edge of the mirror, and an apparent surface error of about 3 μm for a 1 arcsecond angular error.)

We purchased a tracker and developed procedures for measuring the surface of the NST mirror, initially in the lab before starting the loose-abrasive grinding. The basic procedure is to place the tracker ball at different points on the mirror surface and measure their positions. Our initial plan was to fit a paraboloidal surface to these points and determine both the best-fit geometry of the off-axis paraboloid (radius of curvature, off-axis distance and clocking angle) and the departure from the best-fit surface. We found that a better method is to hold the off-axis distance and clocking angle fixed (constrained by measurement of fiducial points at known locations on the mirror) and measure the surface error with respect to the ideal paraboloidal surface. Errors in the geometry are equivalent to low-order aberrations in the optical surface. Table 3 lists the sensitivity of each low-order aberration to errors in geometry. If the mirror geometry is held fixed—i. e., the mirror is constrained to be at the correct off-axis distance and clocking angle, and the radius of curvature is not allowed to vary—we simply measure these aberrations in the surface and treat them as errors to be corrected. This method was preferred especially for loose-abrasive grinding, when we could remove enough glass to correct the aberrations that correspond to errors in the geometry. Later, when we were polishing the mirror and making optical measurements, we did not constrain the mirror's position but adjusted it to minimize the low-order aberrations. We did, however, monitor the mirror's position as described in Section 4.2.

Table 3. Sensitivity of low-order aberrations to errors in mirror geometry. Aberrations are given as Zernike polynomial coefficients in μm, with polynomials normalized to unit rms surface error.

	focus	astigmatism (0°)	astigmatism (45°)	coma (0°)	coma (90°)
radius of curvature: +1 mm	-1.76	0	0	0	0
off-axis distance: +1 mm	0.84	0.60	0	0.08	0
clocking: 1.2 mrad = 1 mm counterclockwise	0	0	-1.3	0	-0.17

We built a small fixture to hold the tracker ball at a fixed distance from the edge of the mirror and a fixed distance from the optical surface, at four positions at 90° intervals around the edge of the mirror. We know the positions

of these four fiducial points in a coordinate system centered on the mechanical center of the mirror. By a coordinate transformation we know their positions in a coordinate system centered on the vertex of the parent paraboloid, assuming the mirror has the correct radius of curvature, off-axis distance and clocking angle. Each scan includes measurements of these four points and a series of at least 100 points on the mirror surface. Sampling the surface takes about 5 minutes in continuous measurement mode (see below) or 10 minutes for stop-and-go measurements. Data are recorded in the tracker's native coordinate system, but any coordinate system would do.

To process the data, we first use the four fiducial points to find the transformation from measured coordinates to parent coordinates, i. e. the transformation that puts these four points at the correct positions in the parent coordinates. Using four points provides some redundancy, giving a least-squares solution and an indication of a significant error in any of the four points. Typical residual errors after the best-fit transformation are on the order of 0.2 mm, consistent with the uncertainty in placing the ball on the mirror. This is more than adequate to define the off-axis distance and clocking angle but not to define the piston, tip and tilt of the surface, so these parameters are allowed to float when the surface data are processed.

Next, we take the coordinate transformation obtained from the four fiducial points and apply it to the surface data, thereby putting the surface data in the parent coordinate system. We then find the departure of each point from the ideal surface. The data contain errors on the order of 100 μm in the form of piston, tip and tilt because of errors in the positions of the fiducial points, and these are ignored. We fit Zernike polynomials to the residual errors, typically using polynomials through 6th degree in radius, and take this polynomial fit as the best representation of the surface.

The tracker can measure on command, taking a single sample or an average of multiple samples of a stationary retroreflector. It can also measure as the retroreflector moves continuously, triggering its own measurements according to a user-defined distance between samples. We found that either method works well for a ground surface. The continuous method requires dragging the steel ball over the surface, and this turned out to be the simplest method for the ground surface. We built a wand, seen in Figure 2, that allows a technician to move the ball over the surface without deflecting the mirror. (The photo at the left of Figure 2 shows wooden blocks taped to the mirror, an early attempt to hold the ball stationary at fixed positions with no significant force on the mirror. This turned out to be completely unnecessary as the ball did not need to be stationary and the wand could be used to move the ball over the surface without deflecting the mirror at the micron level.) We also used the laser tracker in the early stages of polishing before the surface was specular enough for the interferometric measurement. For the polished surface we measured at discrete points with the ball stationary, and modified the wand to include a plastic shield that could be inserted between the ball and the mirror surface when we moved from point to point. We took care never to hold the steel ball over the mirror without having protection in place.

The mirror remains on the polishing turntable for the tracker measurements. The tracker is mounted about 2 m above the mirror on a bridge that is locked in place for each measurement. This arrangement is shown in Figure 3 for a different mirror. We found, by rotating the mirror to different orientations, that the tracker has systematic errors that appear as astigmatism in the mirror surface. This may be related to the fact that we could not perform the recommended calibration measurements with the tracker mounted over the mirror, due to space constraints. We therefore routinely made two measurements, with the mirror rotated 90° between them, in order to average out the astigmatic error.

The tracker measurements guided the loose-abrasive grinding and initial polishing from a measured error of 14 μm rms surface to a measured error of 0.9 μm rms (0.6 μm rms with focus removed). Figure 4 shows tracker data taken near the beginning of loose-abrasive grinding and near the end. The astigmatism in the early measurement was repeatable and was gradually reduced through figuring, using dynamic variations of grinding pressure. All measurements include some power, which was treated as a real error to be corrected by figuring. By the end of loose-abrasive grinding, non-repeatable noise contributed 1-2 μm rms to the measured errors. This noise was eliminated in the polynomial fits that guided the figuring.

The purpose of the tracker measurements was to guide the figuring to an accuracy that would allow optical testing. The first optical measurement easily resolved fringes at 633 nm and is in good agreement with the tracker measurement, as shown in Figure 5. The interferogram at the lower left shows the excellent contrast of the data, the severe distortion caused by the null corrector, and the accuracy of the mirror surface after figuring solely on the basis of laser tracker measurements. Focus, astigmatism and coma are strongly affected by alignment of the mirror in the optical test; with these aberrations removed, the difference between the optical measurement and the polynomial fit to the tracker measurement was 0.5 μm rms surface.
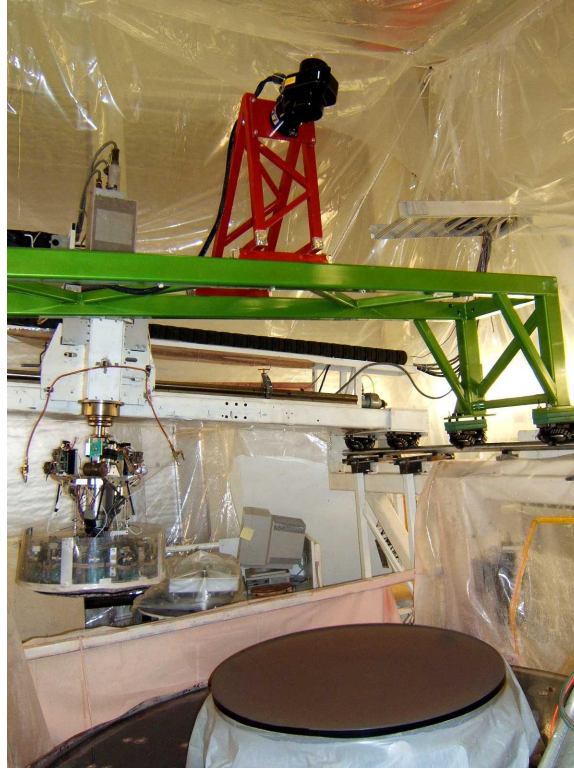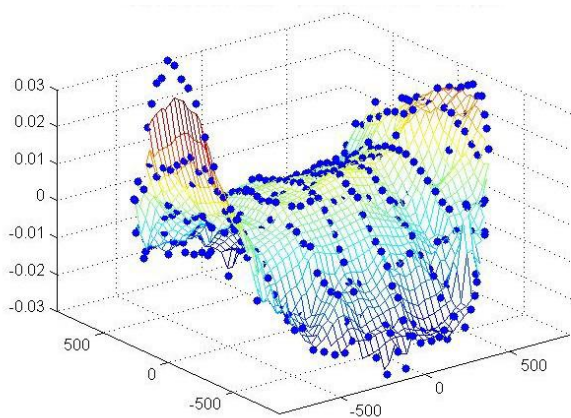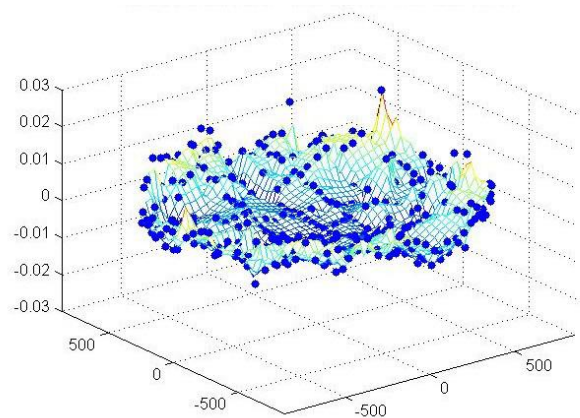
Figure 3. Laser tracker mounted over a 0.95 m mirror. The same arrangement was used for the 1.7 m NST mirror.

31 March 2005: 14 μm rms surface

22 April 2005: 4 μm rms surface

Figure 4. Laser tracker measurements of the NST mirror surface near the beginning of loose-abrasive grinding and near the end. The plots show the departure from the ideal off-axis paraboloid, in mm, with only piston, tip and tilt removed.

We plan to use a laser tracker to measure the ground surfaces of the GMT segments as well. Several sources of error tend to scale with the diameter of the mirror, which would lead to unacceptable accuracy. We are taking several measures to improve the accuracy. One important source of error is rigid-body motion of the segment relative to the tracker (or vice versa) during the scan. Another is variations in refractive index of the air. The laser-tracker measurements will be augmented by four distance-measuring interferometers that stare at fixed retroreflectors near the edge of the GMT segment. This information will be used to correct for physical motion and for large-scale variations in refractive index.

optical measurement: 630 nm rms surface

tracker measurement: 590 nm rms surface
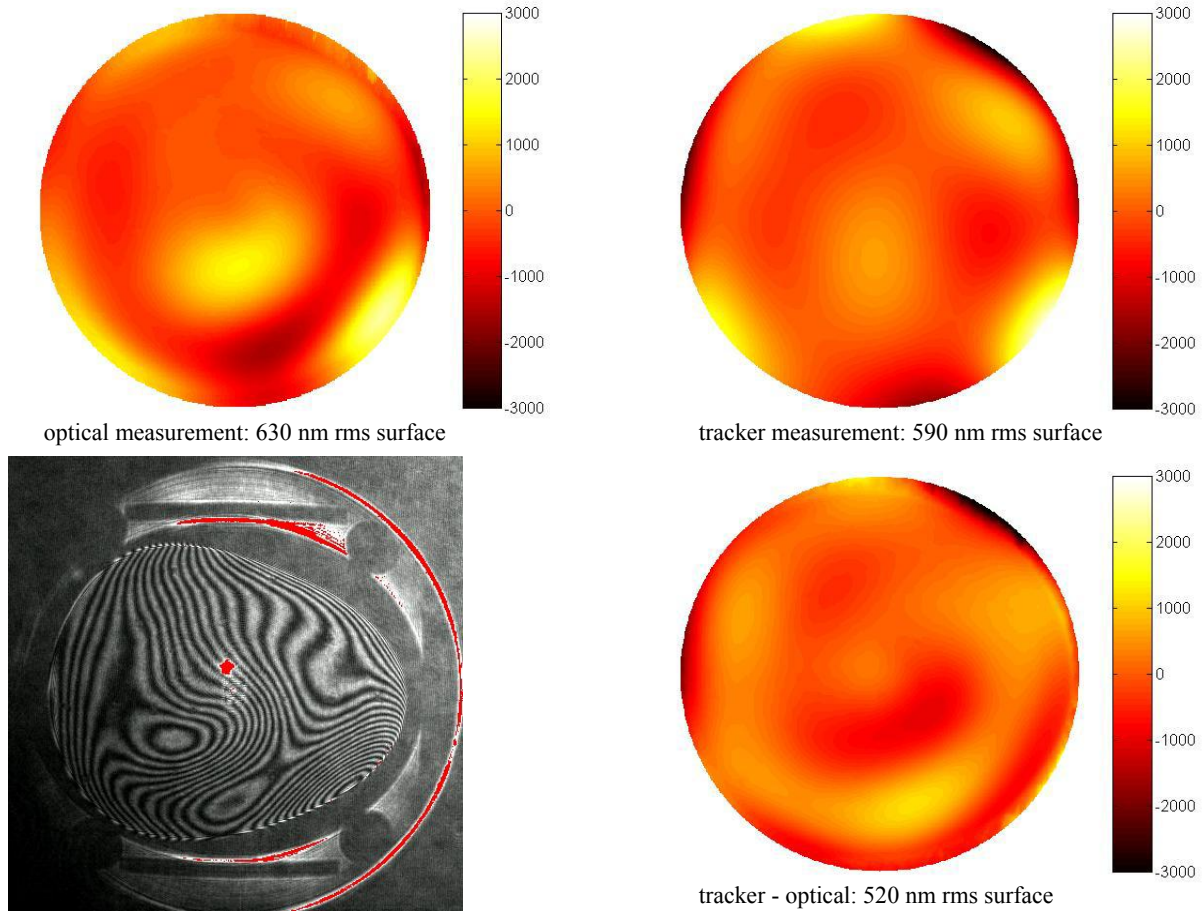

tracker - optical: 520 nm rms surface

Figure 5. Comparison of one of the first optical measurements (two images at left) with laser tracker data taken at the same time (upper right). The difference is shown at lower right. The tracker map is a 6th-degree Zernike polynomial fit to data such as those shown in Figure 4. Focus, coma and astigmatism, which depend strongly on the alignment of the mirror in the optical test, were removed from all three maps. Color bars are labeled in nm of surface.

Errors in the tracker itself can be reduced by calibrating it in a way that matches the geometry of our measurement. To do this, we will measure a small spherical mirror that subtends roughly the same solid angle as the GMT segment, measuring the surface both from its center of curvature and from points displaced from its center of curvature in the two lateral directions. The center-of-curvature measurement is only affected by errors in the distance $\Delta r(\theta,\phi)$, where θ and ϕ are the tracker's elevation and azimuth angles, while the offset measurements are also sensitive to errors in the angles $\Delta\theta(\theta,\phi)$ and $\Delta\phi(\theta,\phi)$. The combination of calibration measurements yields a map of all systematic errors, which can be used to correct the measurements of the GMT surface.

With these improvements, we expect to do better than simply compensate for the increased range of the GMT measurements. The goal is to reduce errors in low-order aberrations, including focus, to less than 0.5 μm rms. This would provide a useful cross-check of the more sensitive optical measurements.

4.2 Optical measurements

The optical measurement is a full-aperture interferometric test that uses a hybrid reflective-diffractive null corrector to compensate for the mirror's 2.7 mm of aspheric departure. The test system is shown in Figure 6. Most of the compensation is done by an oblique reflection off a 0.5 m diameter spherical mirror, and the rest is done by a computer-generated hologram. This test is a prototype for the principal optical test of the GMT segment, although the GMT test requires two spherical mirrors (3.8 m and 0.75 m diameter) to compensate for the 14 mm aspheric departure.
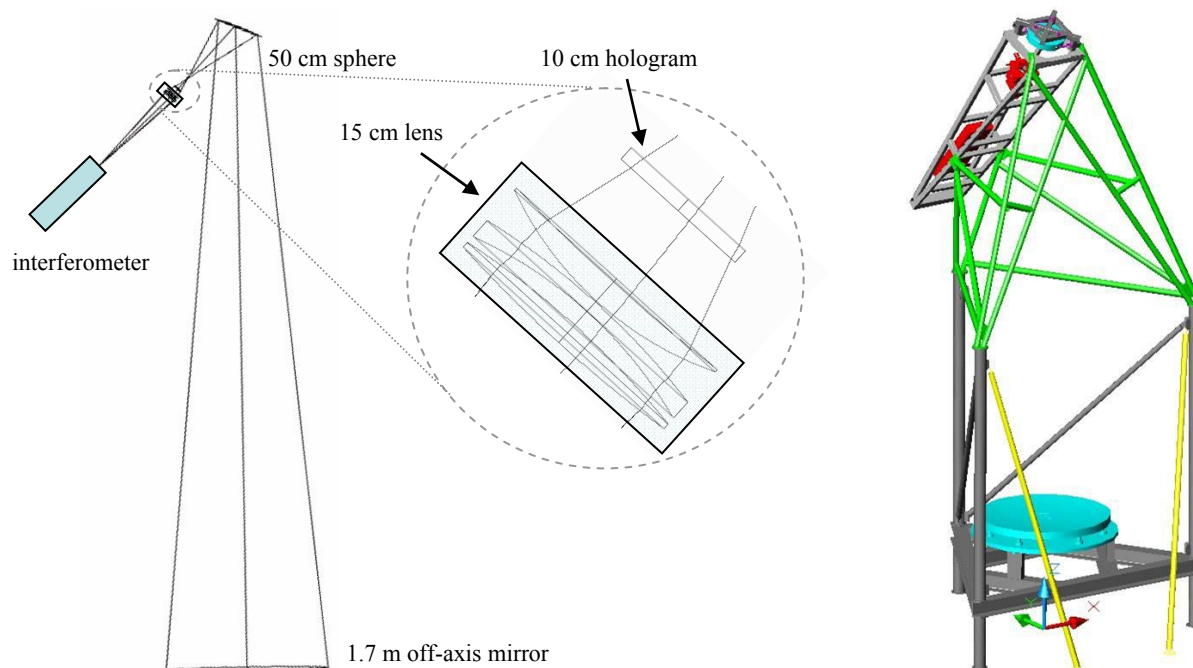
Figure 6. Optical test system for the NST mirror. In the view at left, the optical axis of the parent is 1.84 m to the left of the center of the NST mirror. The blow-up shows a focusing lens and the computer-generated hologram. The view at right shows the tower that holds the test optics.

Alignment of the components of the test is critical, and we have developed alignment techniques that make use of the computer-generated hologram.[10] The tolerance analysis for alignment follows the same method used for the GMT test. It is based on the fact that the mirror will be aligned in the telescope to optimize its reflected wavefront, then several low-order aberrations will be corrected by the mirror's active support system. The tolerance analysis simulates this procedure as follows. For each alignment parameter in turn:

1. The parameter is perturbed, causing a wavefront error that would be imprinted on the NST mirror.

2. The position of the mirror in the telescope is adjusted (in the ray-trace program) to compensate for this wavefront error.

3. Support forces are optimized to minimize the remaining wavefront error.

A more precise statement of step 2 is that the position of the mirror in the telescope is adjusted to minimize the support forces required to correct the wavefront error remaining after realignment. For example, to correct one wave of coma by bending the mirror requires much larger forces than those required to correct one wave of astigmatism. Therefore coma is weighted more heavily than astigmatism in step 2. Optimization of support forces in step 3 uses only low-order bending modes that nearly match the low-order optical aberrations. The bending modes and corresponding actuator forces are calculated from a finite-element model of the mirror.

The tolerance analysis keeps track of the displacement of the mirror from its nominal position in the telescope, the support forces used to correct the residual error after realignment, and the remaining wavefront error after applying the support forces. Table 4 shows the results of this analysis. We are confident that the actual misalignments of the components are less than the values used for Table 4. The effect of alignment errors in the test optics is expected to be a change in off-axis distance by less than 0.5 mm, a clocking of less than 0.1 mrad, correction forces less than 14 N rms, and a residual wavefront error less than 24 nm. The tolerance analysis shown here follows the rules used for the GMT test, in that power in the NST mirror is treated as an error, to be corrected by changing the off-axis distance and applying correction forces. If power, or radius of curvature, is allowed to float, the mirror displacements, correction forces and wavefront errors listed in Table 4 are reduced by 10-20%.

Table 4. Tolerance analysis for alignment of the components of the optical test. The interferometer is the reference for displacements of the components. Tilts are expressed as displacement at the edge of the component. Power in the NST mirror is included as an error.

Component	parameter	tolerance	radial shift compensation	clocking compensation	rms correction force	rms wavefront error
		μm	mm	mrad	N	nm
hologram (100 mm diameter)	axial position	10	0.00	0.00	6.4	5.5
	tilt in x	50	0.01	0.01	5.0	10.9
	tilt in y	50	0.01	0.01	3.0	6.4
spherical mirror (500 mm diameter)	axial position	10	0.17	0	2.0	5.2
	tilt in x	10	0.21	0	6.4	8.4
	tilt in y	10	0	0.09	2.1	2.1
	radius of curvature	100	0.25	0	6.2	9.0
temperature		1 K	0.29	0	5.4	13.5
net change (sum in quadrature)			0.46	0.09	13.9	23.5

For the NST test the most difficult dimensions to maintain are those that involve the position of the spherical mirror with respect to the hologram. We determine these dimensions by measuring the distances between tooling balls with metering rods. One tooling ball is near the hologram and four are in contact with the surface of the spherical mirror. Measuring the distances to 10 μm is challenging, and defining the positions of the balls is more challenging. Because the spherical mirror has a substantial tilt with respect to the axis of the test beam, the distances to the tooling balls depend strongly on the positions of the balls on the surface. The hologram, in addition to correcting the wavefront as part of the null corrector, produces reference wavefronts focused at the centers of each of the five balls. Each ball's position can be adjusted to align it to the reference wavefront.

For the optical test of the GMT segment, we will use similar alignment techniques for the distances between the hologram and the 0.75 m spherical mirror, dimensions that must be held to about 10 μm. The longer dimensions between the two spherical mirrors, and between the 3.8 m sphere and the GMT segment, must be held to about 100 μm, and these will be measured with a laser tracker.

The optical measurements alone do not constrain the geometry of the off-axis mirror. The null corrector produces a wavefront whose shape matches the ideal mirror surface at a precise distance from the null corrector and over a particular 1.7 m aperture. The real mirror is not precisely at the correct position with respect to the null corrector, so the reference wavefront incident on it does not have the ideal shape. The mirror can appear perfect (return a null wavefront) while having significant low-order aberrations. A similar situation holds for axisymmetric mirrors, but there are simple methods that use the mirror's symmetry to establish its position with respect to the null corrector to sub-mm accuracy, which is typically adequate for a telescope.

We use the laser tracker to measure the position of the off-axis mirror with respect to the null corrector. Preliminary data indicate that the measurements are accurate to better than 1 mm in three dimensions. An accuracy of 1 mm out of the roughly 3 m^2 x 7 m volume of the test is not extraordinary, but we are relieved to achieve this given the lack of symmetry and limited mechanical references in the null corrector. For example, the hologram is written on a 100 mm diameter substrate that, mechanically, constrains the geometry strongly in one degree of freedom (displacement perpendicular to the surface) but weakly in two more (tip and tilt, because of the small substrate diameter) and not at all in the other three. The surface of the spherical mirror constrains the geometry in only three degrees of freedom (the position of its center of curvature).

The multiple patterns on the CGH are used to define the geometry of the null corrector, and through its reference wavefronts it optically defines the positions of the five tooling balls that serve as mechanical references for the mirror alignment. We use the laser tracker to measure the positions of the five balls (in arbitrary tracker coordinates). We know the ideal positions of these balls in a coordinate system centered at the vertex of the parent paraboloid. We use the five balls to find the best-fit transformation from the tracker coordinates to the parent coordinates. We then measure the position of the mirror, using its four fiducial points, in the same tracker coordinates and apply the same transformation to obtain the position of the mirror in parent coordinates. This gives us the error in off-axis distance, clocking angle, and axial displacement. The axial displacement causes mainly an error in focus or radius of curvature.

The tracker measurements are made in conjunction with an optical measurement of the mirror figure. The optical test includes focus and other low-order aberrations affected by the position of the mirror. Using the sensitivity of each aberration to position listed in Table 3, we find the desired displacement of the mirror that minimizes these aberrations (more precisely, minimizes the support force required to correct residual errors after realignment). This displacement is added to the displacement measured with the laser tracker to give a net displacement from the ideal geometry, along with a set of support forces and a residual wavefront error.

5. CURRENT STATUS OF THE NST MIRROR

We carried out the loose-abrasive grinding and initial polishing, guided by laser-tracker measurements of the surface, between March and August 2005. While implementing the optical test we encountered a problem in the alignment techniques that limited the accuracy to about 20 μm where 10 μm was desired. The resulting wavefront error was expected to be small so we continued to figure the mirror until January 2006. The alignment problem was resolved in April 2006, and we are now ready to resume figuring with a more accurate optical test. The mirror's surface figure as measured in December 2005 is shown in Figure 7. The measurements show 32 nm rms after removal of some low-order aberrations that will be controlled by the active supports. Further improvement is expected as we continue to polish the surface.
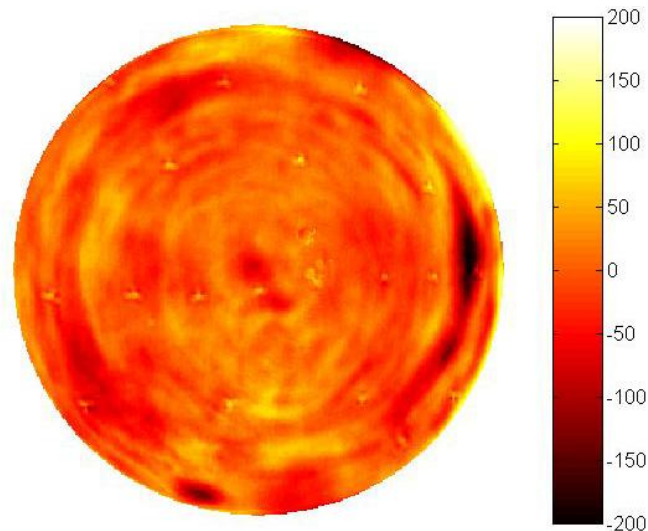

Figure 7. Figure of the NST mirror as of December 2005. Only the 1.6 m clear aperture that will be used in the telescope is shown. Small amounts of low-order aberrations that will be corrected by the active support system have been subtracted. The rms surface error was 32 nm and will improve with further polishing. The color bar is labeled in nm of surface error.

6. SUMMARY

We are figuring the 1.7 m off-axis primary mirror for the New Solar Telescope as part of the technology development for manufacture of the 8.4 m off-axis segments of the GMT. We have developed and demonstrated on the NST mirror many of the techniques that will be used to polish and measure the GMT segments. These include an interferometric measurement with a reflective-diffractive null corrector, accurate measurement of the ground surface

with a laser tracker, and alignment techniques that involve the hologram, metering rods and the laser tracker. The NST mirror is near completion.

REFERENCES

1. M. Johns, R. Angel, S. Shectman, R. Bernstein, D. Fabricant, P. McCarthy and M. Phillips, "Status of the Giant Magellan Telescope (GMT) Project", in *Ground-based Telescopes*, ed. J. M. Oschmann, SPIE 5489, p. 441 (2004).

2. M. Johns, "The Giant Magellan Telescope (GMT)", in *Ground-based and Airborne Telescopes*, ed. L. M. Stepp, Proc. SPIE 6267 (2006).

3. H. M. Martin, J. R. P. Angel, J. H. Burge, B. Cuerden, W. B. Davison, M. Johns, J. S. Kingsley, L. B. Kot, R. D. Lutz, S. M. Miller, S. A. Shectman, P. A. Strittmatter and C. Zhao, "Design and manufacture of 8.4 m primary mirror segments and supports for the GMT", in *Optomechanical Technologies for Astronomy*, ed. E. Atad-Ettedgui, J. Antebi and D. Lemke, Proc. SPIE 6273 (2006; these proceedings).

4. H. M. Martin, R. G. Allen, J. H. Burge, L. R. Dettmann, D. A. Ketelsen, S. M. Miller and J. M. Sasian, "Fabrication of mirrors for the Magellan Telescopes and the Large Binocular Telescope", in *Large Ground-based Telescopes*, ed. J. M. Oschmann and L. M. Stepp, Proc. SPIE 4837, p. 609 (2003).

5. H. M. Martin, R. G. Allen, B. Cuerden, J. M. Hill, D. A. Ketelsen, S. M. Miller, J. M. Sasian, M. T. Tuell and S. Warner, "Manufacture of the second 8.4 m primary mirror for the Large Binocular Telescope", in *Optomechanical Technologies for Astronomy*, ed. E. Atad-Ettedgui, J. Antebi and D. Lemke, Proc. SPIE 6273 (2006; these proceedings).

6. J. H. Burge, "Applications of computer-generated holograms for interferometric measurement of large aspheric optics", in *Optical Fabrication and Testing*, ed. T. Kasai, Proc. SPIE 2576, p. 258 (1995).

7. J. H. Burge, L. B. Kot, H. M. Martin, C. Zhao and R. Zehnder, "Design and analysis for interferometric testing of the GMT primary mirror segments", in *Optomechanical Technologies for Astronomy*, ed. E. Atad-Ettedgui, J. Antebi and D. Lemke, Proc. SPIE 6273 (2006; these proceedings).

8. J. H. Burge, T. Zobrist, L. B. Kot, H. M. Martin and C. Zhao, "Alternate surface measurements for GMT primary mirror segments", in *Optomechanical Technologies for Astronomy*, ed. E. Atad-Ettedgui, J. Antebi and D. Lemke, Proc. SPIE 6273 (2006; these proceedings).

9. C. Denker, P. R. Goode, D. Ren, M. A. Saadeghvaziri, A. P. Verdoni, H. Wang, G. Yang, V. Abramenko, W. Cao, R. Coulter, R. Fear, J. Nenow, S. Shoumko, T. J. Spirock, J. R. Varsik, J. Chae, J. R. Kuhn, Y. Moon, Y. D. Park and A. Tritschler, "Progress on the 1.6-meter New Solar Telescope at Big Bear Solar Observatory", in *Ground-based and Airborne Telescopes*, ed. L. M. Stepp, Proc. SPIE 6267 (2006).

10. R. Zehnder, J. H. Burge and C. Zhao, "Use of computer-generated holograms for alignment of complex null correctors", in *Optomechanical Technologies for Astronomy*, ed. E. Atad-Ettedgui, J. Antebi and D. Lemke, Proc. SPIE 6273 (2006; these proceedings).